REPORT

2021 SCEC Proposal - 21176

Project Title:

Robust Common-Mode Filtering to Best Reduce Uncertainty and Temporal Variability in CGM GPS Velocities

Principal Investigator:

Corné Kreemer

Institutional Affiliation:

Nevada Bureau of Mines and Geology, and Nevada Seismological Laboratory
University of Nevada - Reno

Proposal Category:

A. Data Gathering and Products

Addressing SCEC Science Objectives:

P2. a, P5. c and P.1 a

REPORT

We applied the CMC Imaging approach (Kreemer & Blewitt 2021) to the time-series of all CGPS stations in the western US available from the Nevada Geodetic Lab (NGL) (Blewitt *et al.* 2018). We consider the time interval Jan 1 1994 till Dec 31, 2021. CMC Imaging has proven elsewhere to be the most effective common-mode filtering approach, resulting in significantly reduced scatter in the GPS time-series, and correspondingly the velocity uncertainties as well. The actual velocities will improve as well, particularly for shorter operating stations, as long period signals such as droughts get captured by the common-mode and removed from the time-series.

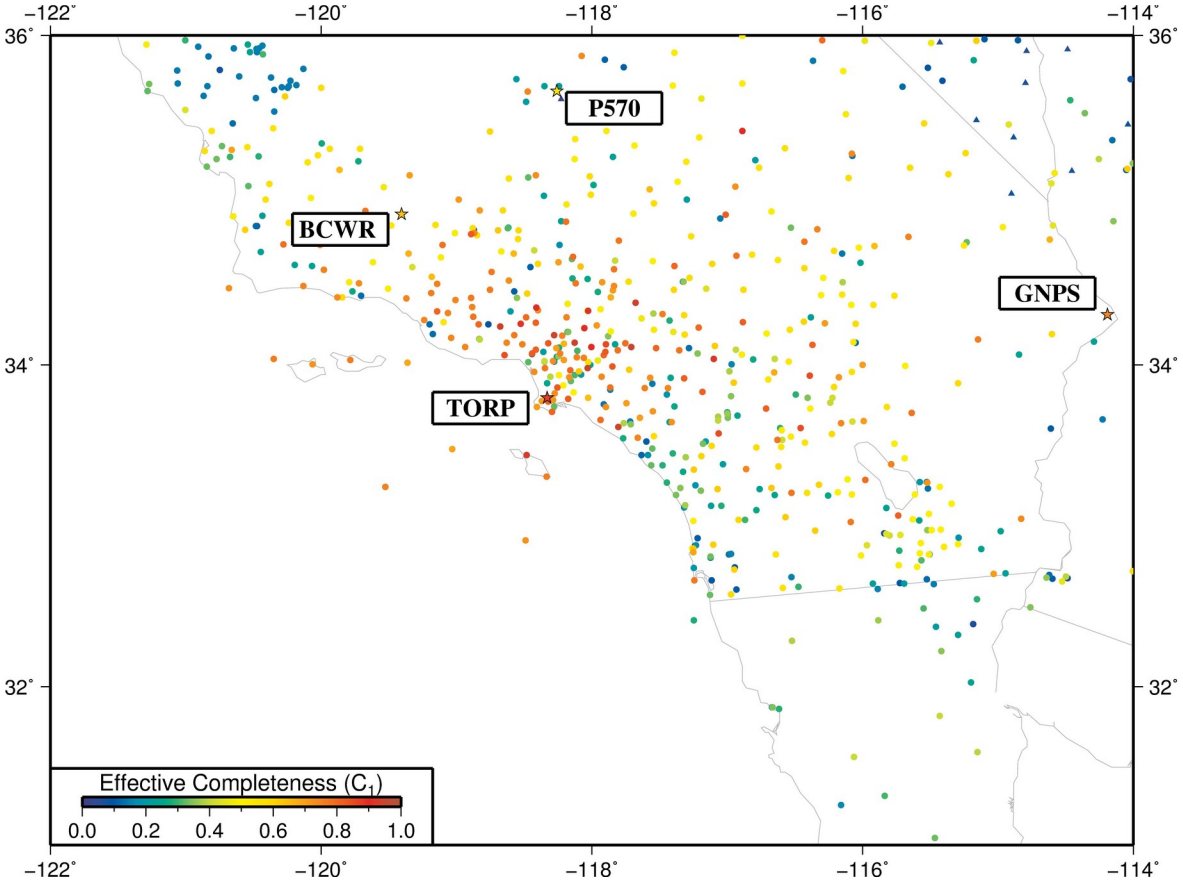

Figure 1 *- Locations of GPS stations considered in southern California, color-coded to their effective completeness between Jan 1, 1994 and Dec 32, 2021. Results for the starred locations are highlighted in other figures.Trangles are stations that had limited data and are not used in the filtering.*

Figure 1 shows GPS stations considered in southern California, color-coded to their effective completeness between Jan 1, 1994 and Dec 32, 2021. Results for the starred locations are highlighted in other figures.

Figure 2-5 show the residual time-series for the original and filtered time-series for stations TORP, GNPS, BCWR and P570, respectively. The figures also indicates the dramatic decrease in RMS misfit values. The filtering removes the “hump” in 2002-2004 seen in TORP (Fig 2.). For GNPS (Fig. 3), a long transient signal in the north component caused the offset during the 2010 El Mayor-Cucapah to not be fully removed. After the filtering removes any common signals in the region, the offset is now properly estimated and removed. For

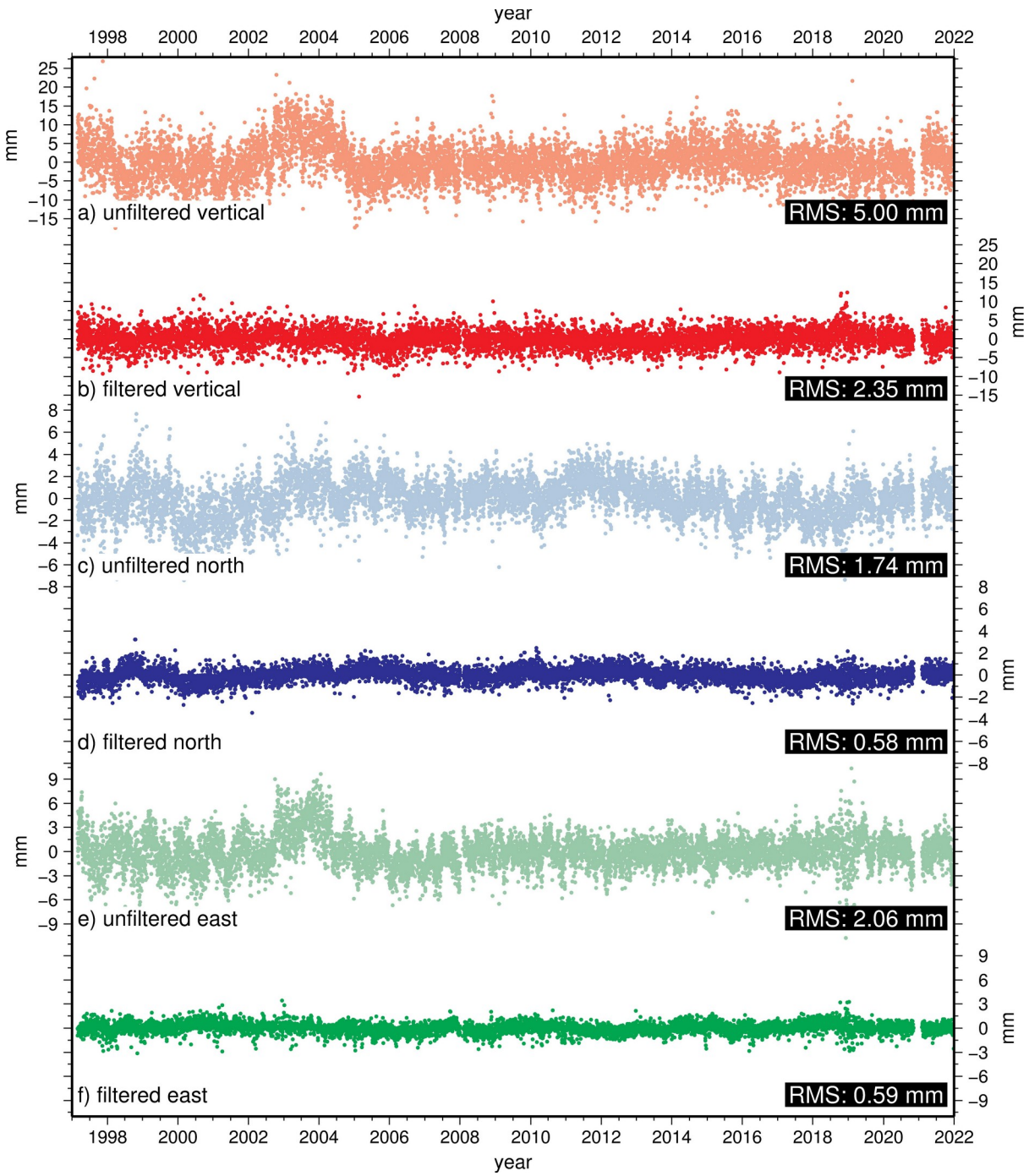

Figure 2 *– Residual time-series in vertical, north and east directions, either with or without common-mode filtering. Shown RMS values reflect scatter in the time-series. This is for station TORP.*

Table 1. Median RMS error of residual time-series for original and filtered case, including percentage reduction

	RMS East (mm)	RMS North (mm)	RMS Up (mm)
Unfiltered	1.73	1.56	4.98
Filtered	0.77 (55.2%)	0.81 (47.7%)	2.71 (45.3%)

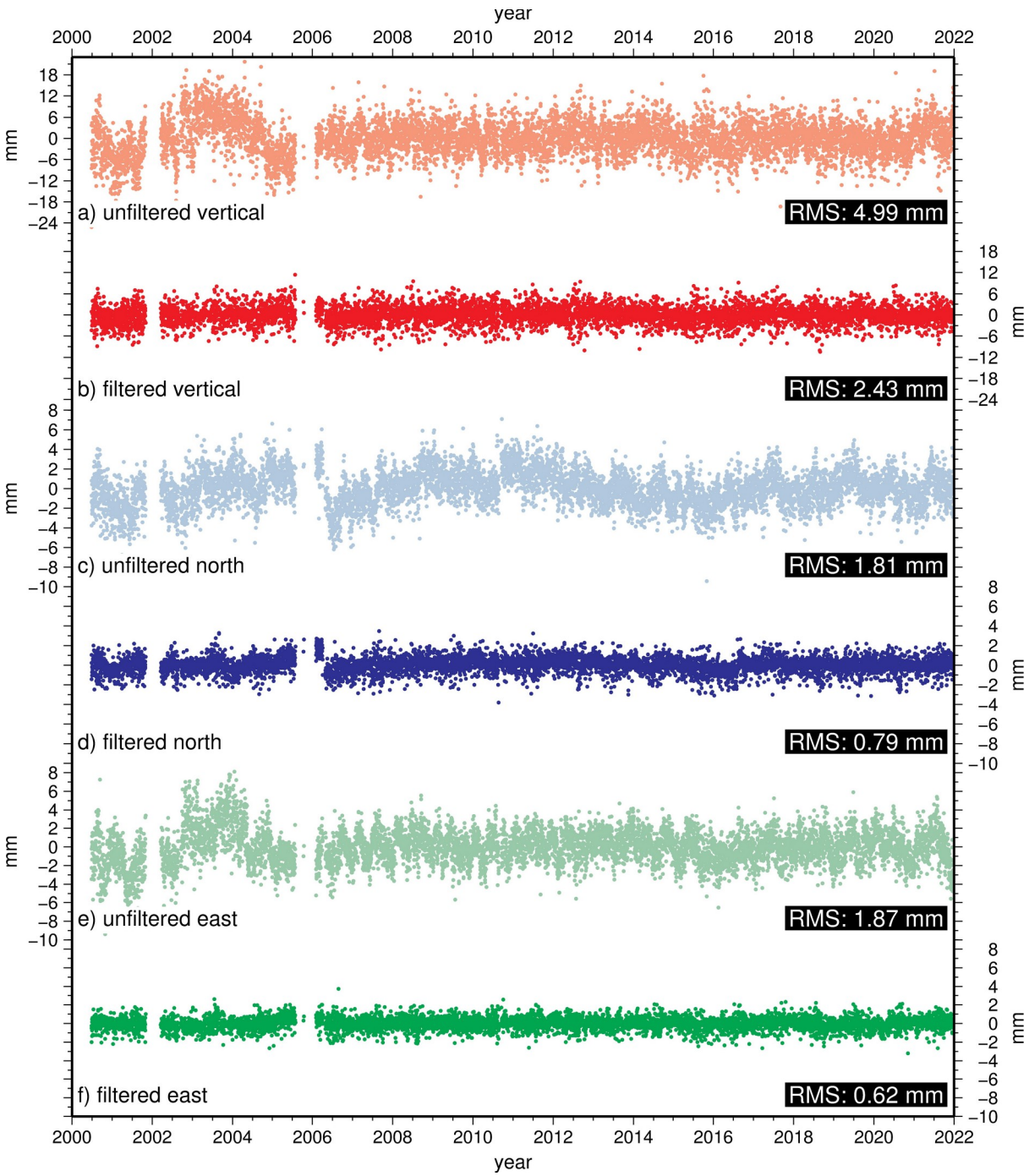

Figure 3 *– Same as figure 2 but for station GNPS.*

BCWR (Fig 4.) and P570 (Fig 5), an uplift signal during the 2011-2016 can be seen. This is removed after filtering.

Figures 2-5 show representative stations for the RMS reduction. Table 1 shows the median value for the entire WUS. Suprisingly, unlike other students, we do not find the highest reduction in the vertical component (which is most affected by common-mode hydrologic loading), but in the east component. The reason for this is not yet clear, but may be due to the filtering out of the slow-slip events in Cascadia, which notably affects the east component. This requires more investigation.

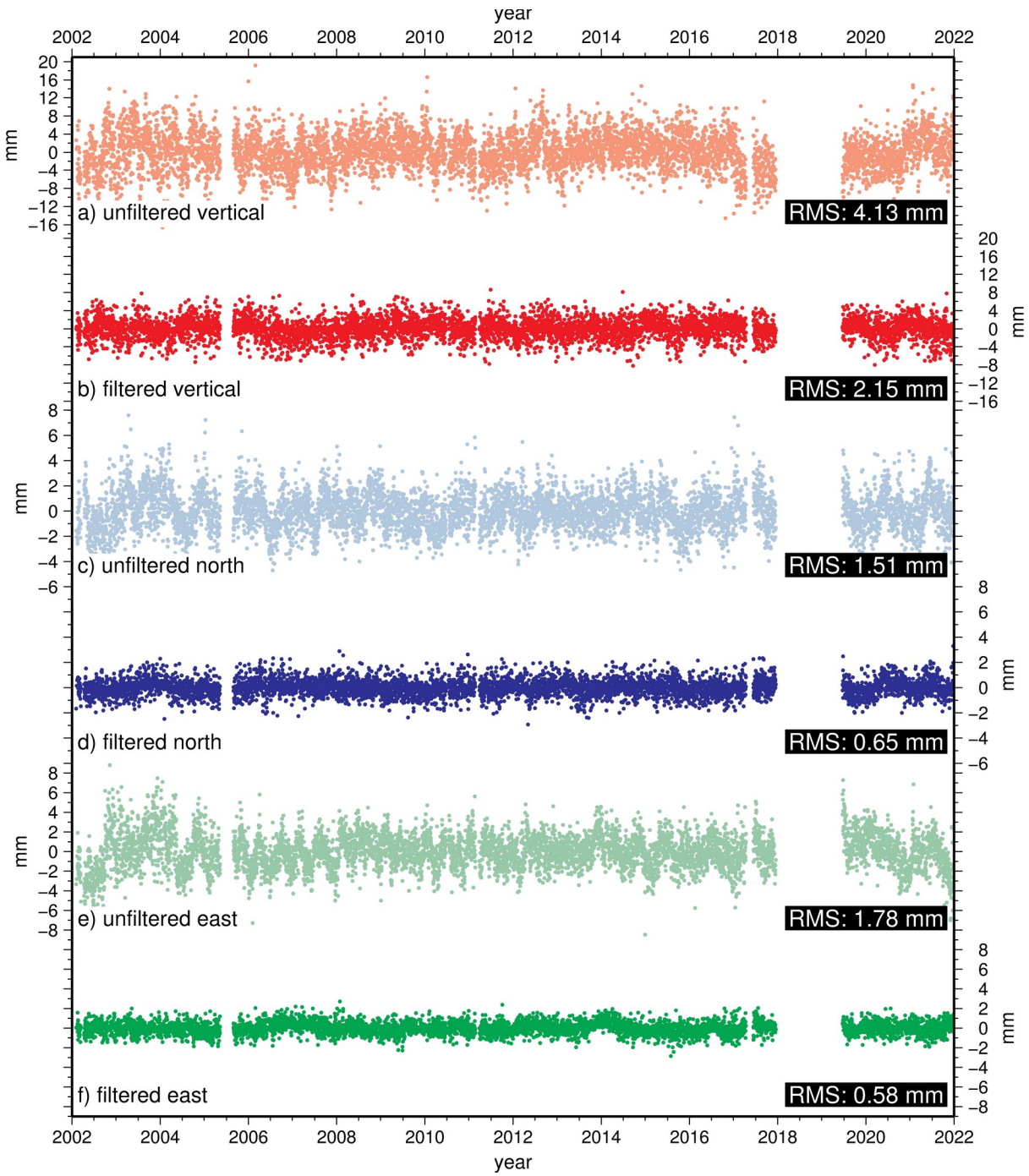

Figure 4 *– Same as figure 2 but for station BCWR.*

The RMS reduction generally translates into a simular percentage reduction in velocity uncertainty (Fig.6). The reason for this is because we estimated velocities and their uncertainties using the MIDAS algorithm (Blewitt *et al.* 2016). MIDAS trend estimation and associated uncertainty is based on applying median statistics on each pair of positions one year apart.

The common-mode filtering removes signals with different frequencies. The long-period frequency signals (e.g., related to drought) particularly affect the velocity estimation, particularly for shorter time-series. To illustrate the effect of filtering, we show in Figure 7 for

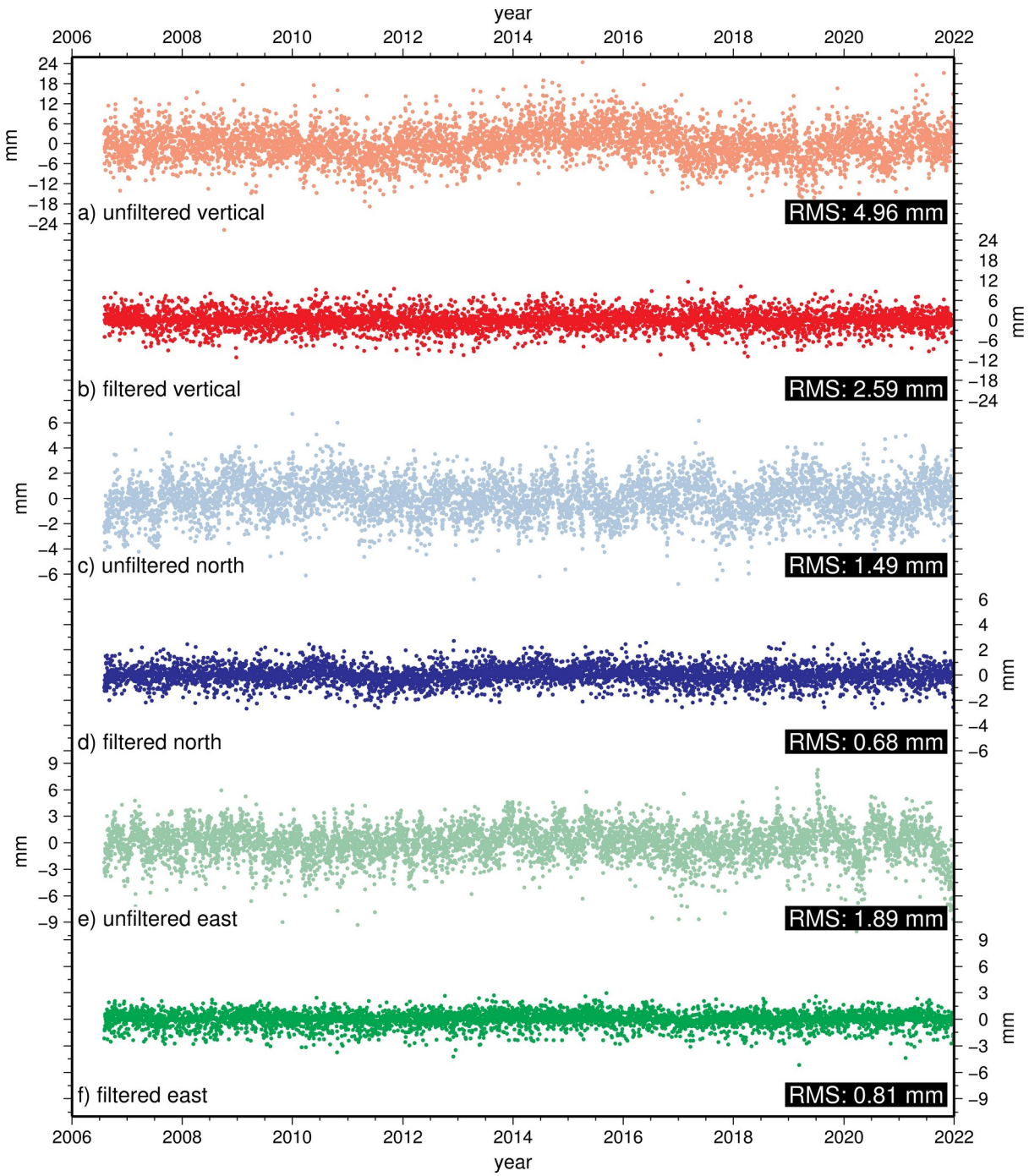

Figure 5 *– Same as figure 2 but for station P570.*

one of the long-running stations (TORP) the temporal variation in velocity derived from the unfiltered and filtered time-series and shown relative to the long-term trend. The short-term and long-term velocities and velocity uncertainties are each estimated using the MIDAS algorithm . For this example we estimate the velocity for a 2.5-year window of the time-series that steps through the time-series with steps of 0.2 years. The scatter in these velocity time-series is shown by the RMS error (calculated using the MAD) and it is clear that the variation in the time-series is substantially reduced for the filtered case. Indeed, the reduction is proportional to the reduction in the uncertainty of the long-term trend (shown for reference), which is not surprising given how MIDAS uncertainties are calculated.

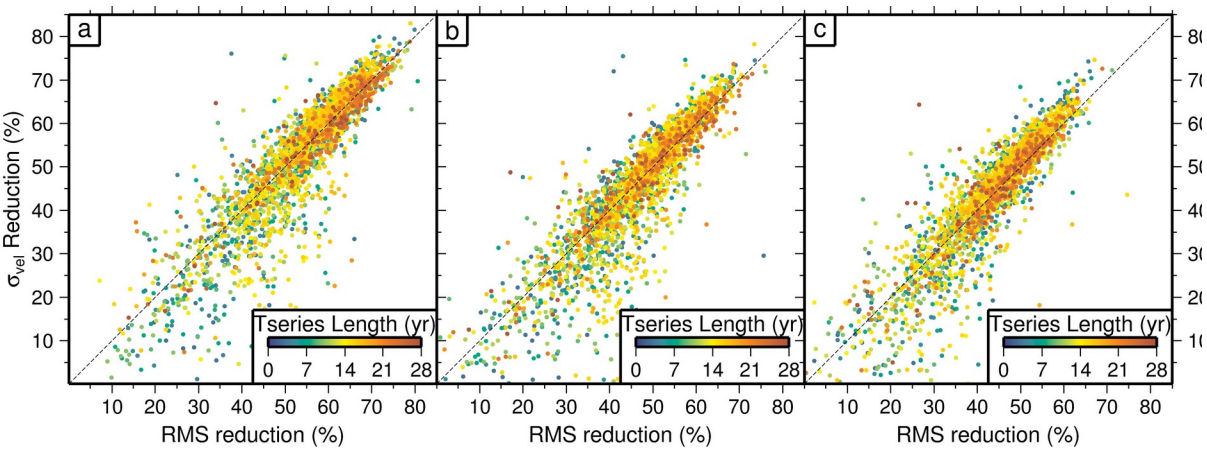

Figure 6 *- Reduction in RMS versus reduction in MIDAS uncertainty of velocities calculated by comparing results when using filtering (using CMC Imaging) relative to not filtering. Values are colour-coded based on length of the time-series. a) East, b) North, c) Up.*

For illustration, the actual common-mode time-series for the 4 stations presented are shown in Figure 8. We focus here on the up component. The hump from 2002-2004 can be seen across southern California, and we see in fact all across the western and central US. We have no explanation for it. The uplift trend from 2011-2016 is only evident for BCWR and P570, and can be attributed to the drought then. The lower amount of snow on the Sierras and the increased contemporary water pumping in the Great Valley caused bedrock stations to move upward.

More work is needed to understand the common-mode signal. Also, given the strong effect on velocity estimation, the analysis needs to be expanded to campaign time-series, for which the effect of filtering is expected to be be largest.

Funds for this project helped with the time-series analysis that ultimately fed into the work presented by Kreemer and Young (2022). A grad student (Zachary Young) was supported to analyze time-series and do the filtering, which went into a publication focused on strain accumulation in the southern Nevada area (Young *et al.* 2023).

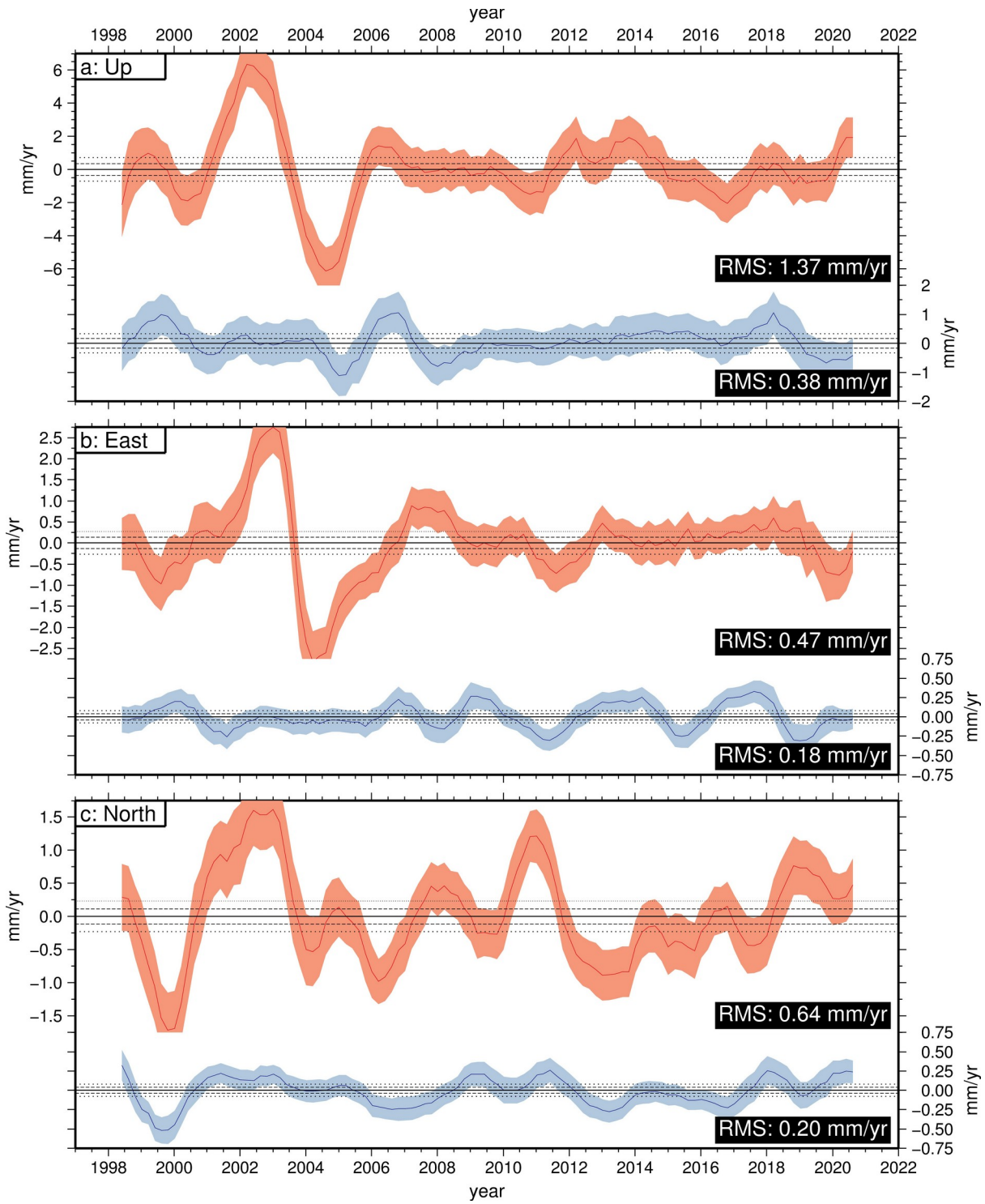

Figure 7. *- Example time-series for station TORP of MIDAS velocity for 2.5 year periods centred on a moving window for every 0.2 years. Red/blue line and outline are velocity and one standard deviation for unfiltered and filtered time-series, respectively. Velocities are plotted relative to long-term trend and, for reference, the dashed and dotted lines are 1 and 2 standard deviations in that trend, resp. Scatter is indicated by the RMS statistic.*

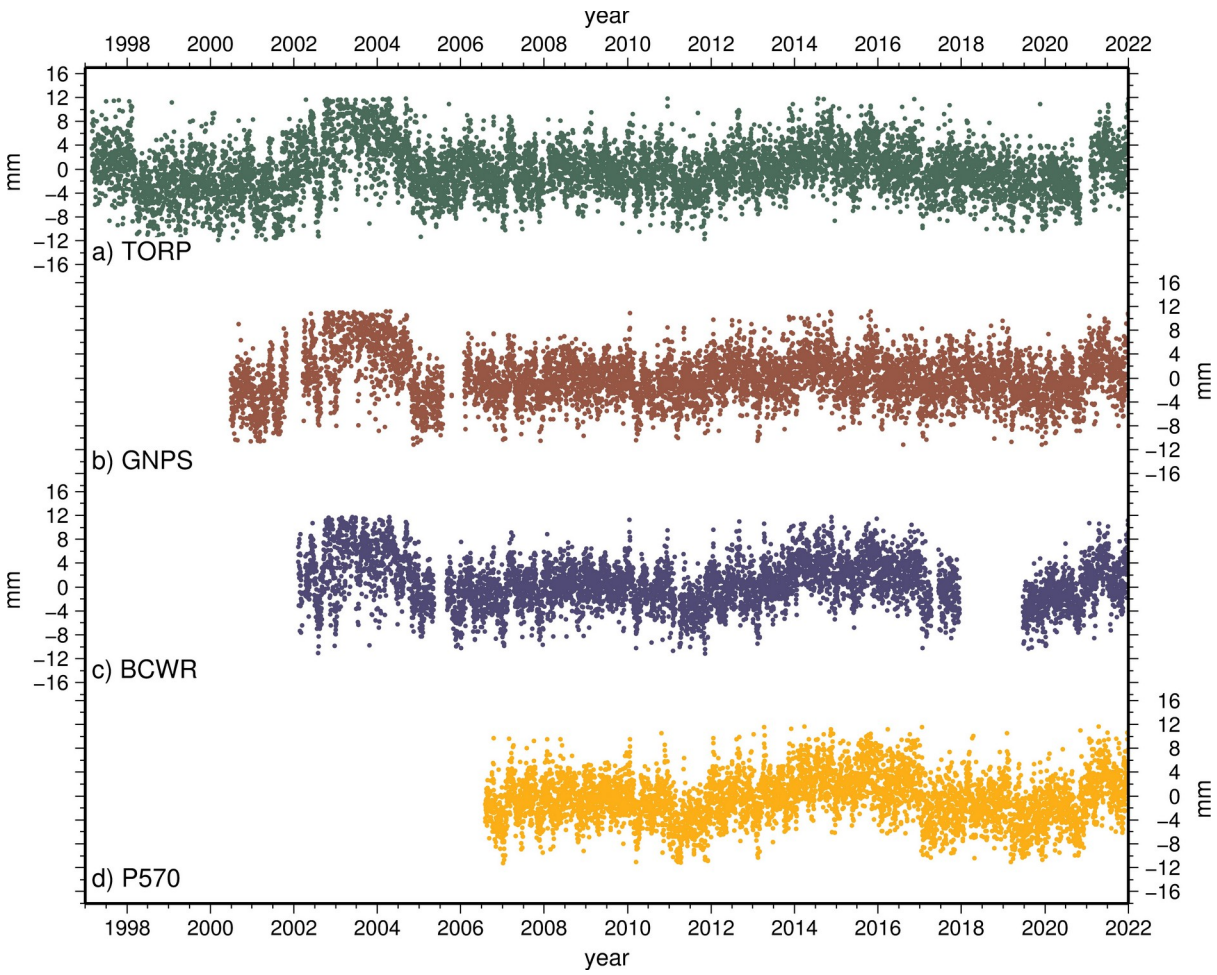

Figure 8. *- Common-mode time-series for the up direction for the 4 stations shown in Fig. 1.*

References

Blewitt, G., Hammond, W.C. & Kreemer, C., 2018. Harnessing the GPS data explosion for interdisciplinary science. *Eos*, **99**. doi:10.1029/2018EO104623

Blewitt, G., Kreemer, C., Hammond, W.C. & Gazeaux, J., 2016. MIDAS robust trend estimator for accurate GPS station velocities without step detection. *J. Geophys. Res. Solid Earth*, **121**, 2054–2068. doi:10.1002/2015JB012552

Kreemer, C & Young, Z.M., 2022. Crustal strain rates in the Western U.S. and their relationship with earthquake rates. *Seismological Research Letters*, **93**, 2990–3008.

Kreemer, Corné & Blewitt, G., 2021. Robust estimation of spatially varying common-mode components in GPS time-series. *J Geod*, **95**, 13. doi:10.1007/s00190-020-01466-5

Young, Z.M., Kreemer, C., Hammond, W.C. & Blewitt, G., 2023. Interseismic Strain Accumulation Between the Colorado Plateau and the Eastern California Shear Zone: Implications for the Seismic Hazard Near Las Vegas, Nevada. *Bulletin of the Seismological Society of America*, **113**, 856–876.